IJE TRANSACTIONS C: Aspects Vol. 27, No. 3, (March 2014) 487-498

International Journal of Engineering

Journal Homepage: www.ije.ir

Stability Analysis in Parametrically Excited Electrostatic Torsional Micro-actuators

B. Abbasnejad, R. Shabani*, G. Rezazadeh

Mechanical Engineering Department, Urmia University, Urmia, Iran

PAPER INFO

Paper history:
Received 06 June 2013
Received in revised form 13 August 2013
Accepted 22 August 2013

Keywords:
MEMS
Micro-mirror
Electrostatic Actuation
Parametric Oscillation
Perturbation Method

ABSTRACT

This paper addresses the static and dynamic stabilities of a parametrically excited torsional micro-actuator. The system is composed of a rectangular micro-mirror symmetrically suspended between two electrodes and acted upon by a steady (*dc*) while simultaneously superimposed to an (*ac*) voltage. First, the stability of the system subjected to a quasi-statically applied (*dc*) voltage is investigated, where the pull-in instability, equilibrium positions, and bifurcation points of the system are determined. Then by superimposing an (*ac*) voltage and extracting a Mathieu type governing equation the effects of (*ac*) component on the stability of the system is investigated. By varying excitation parameters (steady (*dc*) voltage and time-dependent amplitude of (*ac*) excitation), transition curves and the stability margins of the micro-mirror are demonstrated. Theoretically obtained margins are checked by means of numerical simulations. The results show that superimposing the harmonic (*ac*) component could have a stabilizing effect and allow an increase of the steady (*dc*) component beyond the pull-in value. These results could be used in design of micro-actuators.

doi: *10.5829/idosi.ije.2014.27.03c.17*

1. INTRODUCTION

Recently there has been a growing interest in the development of micro-electro-mechanical systems 'MEMS' in particular micro-opto-electro-mechanical systems 'MOEMS'. Electrostatic torsional micro-mirrors have been widely used as an important type of actuators in MOEMS. They can be classified in four groups based on their motion: deformable micro-mirrors [1], movable micro-mirrors [2], piston type [3], and torsional micro-mirrors [4]. Torsional micro-mirrors are used for reflecting light beams to a desired direction in many engineering devices such as projection display systems [5], optical scanners [6], and confocal microscopes [7]. They are also utilized in telecommunication field as optical switches and optical cross-connects [8]. In addition, they have been used as virtual masks (for DNA patterning) [9, 10], micro lenses, micro gratings, and optical waveguides in MOEMS [11].

In the aforementioned applications, besides its flatness and reflectivity, performance of the micro-mirror depends on the mirror size, natural frequency, operating voltage, and rotation angle. Consequently, many researchers devoted their time to investigating the dynamic response and instability of these systems, where the pull-in is the most important type of instability that occur in electrostatically actuated micro-mirrors. Fischer et al. investigated the static and dynamic behavior of micro-mirrors using finite element analysis and clarified the dependency of natural frequency on the squeeze film conditions [12]. Taking into account the finite tilting angle and using general Reynolds equation, Bao et al. [13] proposed an analytical model to calculate the squeeze-film effects. Effects of intermolecular Van der Waals and Casimir forces on the static and dynamic responses of torsional actuators have been also investigated by some researchers. Influence of damping effects were studied by Lin and Zhao [14], where the intermolecular forces effects were considered. Gusso et al. studied the effects of Casmir force on the response of micro-mirrors [15]. Guo and Zhao studied the effects of these forces on the static and dynamic behavior of electrostatic torsional micro and nano-electromechanical actuators [16, 17]. In another study, they also investigated the effect of Casmir and capillary forces on the stability of the

*Corresponding Author Email: r.shabani@urmia.ac.ir (R. Shabani)

micro-mirrors [18]. Bifurcation analyses have also been done on the dynamics of nano-electromechanical actuators, where the Hopf and saddle node bifurcations were detected [19]. In the analysis of micro-mirrors, besides the torsional mode bending mode may also affect the response. But, due to ignoring the coupling effects, the related works are not addressed here. Referring to the above mentioned researches, the main focus in the previous studies has been on the eigen-frequency analysis or developing the response of the system to step excitations or mechanical shocks.

However, in some applications such as micro scanners, the micro-mirror may be excited by a harmonic (*ac*) component superimposed on the steady (*dc*) voltage [20-22]. Therefore, the stability of the system due to imposing (*ac*) components could be important. Stabilizing effects of a (*dc*) component have been investigated in some MEMS structures. Imposing a harmonic component using piezoelectric layers, Azizi et al. [23] investigated the stability of a micro-beam actuated by electrostatic voltage. Employing parametric excitations, they showed stability margins due to variations of (*ac*) excitation parameters. Krylov et al. [24] investigated stability margins of a micro-beam actuated symmetrically by a pair of electrostatic actuators (double electrode micro-beam). Employing electrostatic (*ac*) excitation, they extracted Mathieu type governing equation and studied the (*ac*) and (*dc*) components on the stability margins of the system. Moreover, based on variational iteration method, Rezazadeh et al. [25] studied the parametric excitations of a micro-beam actuated symmetrically by a pair of electrostatic actuators and specified it's stability margins. Rhoads et al. [26]studied a double electrode micro-beam which couples the inherent benefits of a resonator with purely-parametric excitation with a simple geometry. They analyzed the local nonlinear response characteristics of the proposed micro-beam. Their results showed that the (*ac*) voltages could have a stabilizing effect and permits an increase of the steady (*dc*) component actuation voltage beyond the pull-in value. Detailed information related to parametric excitations of Mathieu equation has been presented in [27].

In micro and nano applications, the thickness of elements is typically on the order of microns and sub-microns. At this scale, size effect could affect the results [28, 29]. On the other hand, Sadeghian et al. [30, 31] showed that for silicon beams with thickness greater than $1\mu m$, the effective Young's modulus reaches an asymptotic value equal to its macro-scale value (see also experimental results reported by [32-35]). Accounting for the thickness of torsional beams considered in this study, the results will not be affected by size.

In this paper, the stability of a micro-mirror actuated symmetrically by two electrostatic electrodes are investigated. At first, by imposing steady (*dc*) voltage the static stability of the system is studied, where the pull-in instability, equilibrium positions and bifurcation points of the micro-mirror are determined. Then, assuming different initial conditions, the micro-mirror trajectories are plotted in the phase plane, where the attraction zones of each point is specified. The results are compared with those of a micro-mirror excited by a single electrode. In the next stage, by superimposing a harmonic (*ac*) component and driving a Mathieu type governing equation, the stability margins are plotted and effects of excitation parameters on stability of the system is investigated. Stability of the theoretically obtained regions is verified using numerical Runge-Kutta integration method. Finally, the transition curves in conventional parameters plane (δ- ε) are mapped into the physical parameters space (V_{dc}- V_{ac}), where the stability is investigated in the vicinity and beyond the static pull-in voltage V_{sp}. The results show that the superimposing harmonic (*ac*) voltages could have a stabilizing effect and permits an increase of the steady component V_{dc} voltage beyond the pull-in value.

2. MATHEMATICAL MODELING

A schematic view of a micro-mirror actuated by electrostatic electrodes is shown in Figure 1. The micro-mirror may be actuated by only one electrode (Figure 1b), or by two symmetrically parallel electrodes (Figure 1c). The micro-mirror plate is suspended by two torsional micro-beams with length *l*, width *w*, and thickness *t*. The length and width of the micro-mirror plate are denoted by *L* and *a*, respectively, and the initial gap separating the micro-mirror and electrode plates is denoted by *D*.

By applying a voltage to the system, the micro-mirror will rotate around its center axis producing an angular deflection in the micro-beams. The equation for the torsional vibration of the micro-mirror with moment of inertia I_t is stated by [22]:

$$I_t\ddot{\varphi} + K_t\varphi = M_{elec}(\varphi, V)$$
$$K_t\varphi = 2\frac{GJ_p}{l}\varphi \quad (1)$$

where K_t, G and J_p are torsional stiffness, shear modulus, and area moment of inertia of the beams, respectively. The overall electrostatic torque acting on the mirror for single electrode and double electrode actuation is specified as [22]:

$$M^1_{elec}(\varphi, V) = \frac{1}{2}\varepsilon LV^2\left[\int_0^a \frac{rdr}{(D - r\sin\varphi)}\right] \quad (2a)$$

$$M^2_{elec}(\varphi, V) = \frac{1}{2}\varepsilon LV^2\left[\int_0^a \frac{rdr}{(D - r\sin\varphi)} - \int_0^a \frac{rdr}{(D + r\sin\varphi)}\right] \quad (2b)$$

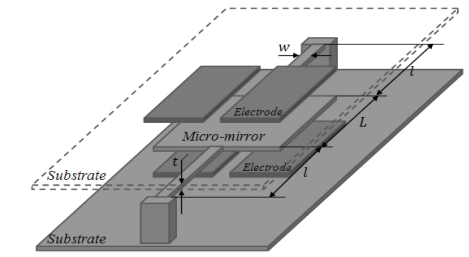

(a)

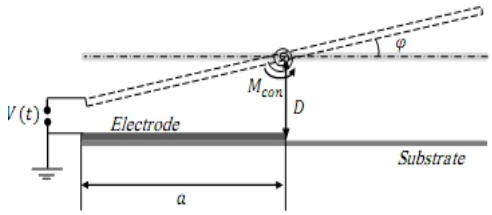

(b)

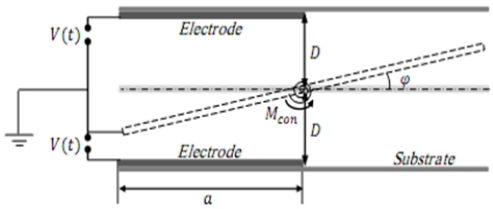

(c)

Figure 1. Schematic view of an electrostatic micro-mirror, (a) 3-D isometric view, (b) cross-sectional view of single electrode actuation, (c) cross-sectional view of double electrode actuation

where ε and V denote the electric permittivity and the applied voltage respectively. By defining the dimensionless parameters,

$$\varphi_0 = \frac{D}{a}\ ;\ \Gamma = \frac{\varphi}{\varphi_0}\ ;\ \sin\varphi \cong \varphi\ ;\ \sin\varphi_0 \cong \varphi_0 \tag{3}$$

the electrostatic torque can be rewritten as:

$$M^1_{elec}(\gamma, V) = \frac{1}{2}\varepsilon L V^2 \frac{a^2}{D^2}\frac{1}{\gamma^2}[\frac{\gamma}{1-\gamma} + \ln(1-\gamma)] \tag{4a}$$

$$M^2_{elec}(\gamma, V) = \frac{1}{2}\varepsilon L V^2 \frac{a^2}{D^2}\frac{1}{\gamma^2}\{[\frac{\gamma}{1-\gamma} + \ln(1-\gamma)] - [\frac{-\gamma}{1+\gamma} + \ln(1+\gamma)]\} \tag{4b}$$

In the case of double electrode actuation, the governing equation can be written as:

$$I_t\ddot{\gamma} + K_t\,\gamma = \frac{1}{2}\varepsilon L\frac{a^3}{D^3}\{T_1(V,\gamma) - T_2(V,\gamma)\} \tag{5}$$

where

$$T_1(V,\gamma) = \frac{V^2}{\gamma^2}[\frac{\gamma}{1-\gamma} + \ln(1-\gamma)] \tag{6a}$$

$$T_2(V,\gamma) = \frac{V^2}{\gamma^2}[\frac{-\gamma}{1+\gamma} + \ln(1+\gamma)] \tag{6b}$$

By expanding the dimensionless electrostatic torques (T_1, T_2) up to second order, the relationship for torque values are obtained as:

$$T_i(V,\gamma) = T_i(V_{dc},0) + \frac{\partial T_i}{\partial V}\Big|_{V_{dc},0}\delta V + \frac{\partial T_i}{\partial \gamma}\Big|_{V_{dc},0}\delta\gamma + \frac{1}{2!}\left(\frac{\partial^2 T_i}{\partial\gamma\partial V}\Big|_{V_{dc},0}\delta V\delta\gamma\right) + \frac{1}{2!}\left(\frac{\partial^2 T_i}{\partial V^2}\Big|_{V_{dc},0}(\delta V)^2\right) + \frac{1}{2!}\left(\frac{\partial^2 T_i}{\partial\gamma^2}\Big|_{V_{dc},0}(\delta\gamma)^2\right) + \ldots \tag{7}$$

in which δV is the time-dependent alternating voltage $\delta V = V_{ac}\cos(\omega t)$ and V_{dc} the constant bias voltage. Upon neglecting higher order terms in Equation (7) and inserting it into Equation (5), the following parametric equation with a time-dependent component is obtained:

$$\ddot{\gamma} + [1 - \frac{1}{K_t}(\frac{1}{2}\varepsilon L(\frac{a}{D})^3)(1.334V_{dc}^2 + 1.334V_{dc}V_{ac}\cos(\omega t))]\gamma = 0 \tag{8}$$

By applying transformation $\tau^* = \omega_0 t$ and introducing the following parameters

$$\Omega = \frac{\omega}{\omega_0};\ H = \frac{1}{K_t}(\frac{1}{2}\varepsilon L(\frac{a}{D})^3)\ ;\ \delta^* = (1 - 1.334HV_{dc}^2)$$
$$\epsilon^* = -1.334HV_{dc}V_{ac}\ ;\ \tau = \frac{1}{2}\Omega\tau^*\ ;\ \frac{d^2\gamma}{d\tau^2} = \ddot{\gamma} \tag{9}$$
$$\delta = 4\delta^*/\Omega^2, \epsilon = 2\epsilon^*/\Omega^2$$

governing equation of the system is stated as:

$$\ddot{\gamma} + (\delta + 2\epsilon\cos(2\tau))\,\gamma = 0 \tag{10}$$

Equation (10) is in the form of Mathieu equation with time-dependent harmonic coefficient, where its stability can be investigated. It should be noted that in micro and nano applications the size effect could change the analysis results. Sadeghian et al. [30,31] demonstrated that there is a strong size-dependency as the characteristic dimensions of the structure approach the material length-scale parameter. However, they showed that for silicon beam thickness greater than $1\mu m$, the effective Young's modulus reaches an asymptotic value equal to its macro-scale value. Figures 2 and 3 show the evolution of experimentally evaluated modulus of elasticity for silicon made structures as reported by them. Therefore, accounting for the thickness of torsional beams considered in this study (Table 1 in numerical results section), analysis results will not be affected by size.

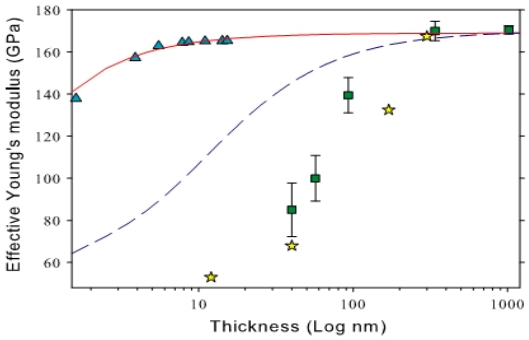

Figure 2. Measured effective Young's modulus of silicon nano-cantilevers for different thicknesses (taken from reference [30]).

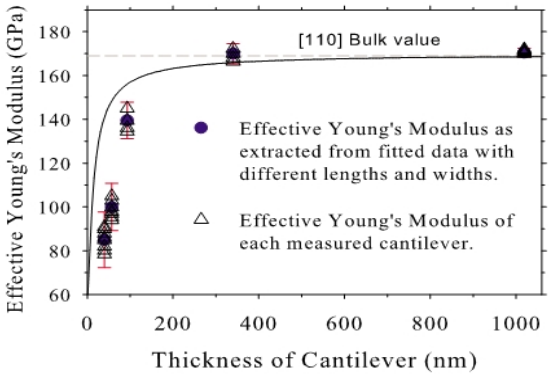

Figure 3. Measured effective Young's modulus of silicon nano-cantilevers for different thicknesses (taken from reference [31]).

3. STABILITY ANALYSIS

3. 1. Static Stability Static stability of the system requires that the action of the applied electrostatic torque ($M_{elec}(\gamma,V)$) be neutralized by the opposite action of elastic restoring torque of the torsional beams ($M_{con}(\gamma)=K_t\gamma$). The equilibrium condition is stated by defining Φ as the following net applied torque:

$$\Phi(\gamma,V)=M_{con}(\gamma)-M_{elec}(\gamma,V)=0 \tag{11}$$

Substituting Equation (4a) and (4b) into Equation (11), the equilibrium equation for single and double electrode actuation can be rewritten respectively as:

$$\gamma^3-HV^2\left\{\left[\frac{\gamma}{1-\gamma}+\ln(1-\gamma)\right]\right\}=0 \tag{12a}$$

$$\gamma^3-HV^2\left\{\left[\frac{\gamma}{1-\gamma}+\ln(1-\gamma)\right]-\left[\frac{-\gamma}{1+\gamma}+\ln(1+\gamma)\right]\right\}=0 \tag{12b}$$

Solving Equations (12a) and (12b) gives the equilibrium points where their stabilities depends on the sign of $\partial\Phi/\partial\gamma<0$. An equilibrium point is stable if $\partial\Phi/\partial\gamma<0$, while it is unstable if $\partial\Phi/\partial\gamma>0$. Therefore, the stability condition for each case is:

$$\frac{\partial\Phi}{\partial\gamma}=3\gamma^2-HV^2\left(\frac{\gamma}{(1-\gamma)^2}\right)=0 \tag{13a}$$

$$\frac{\partial\Phi}{\partial\gamma}=3\gamma^2-4HV^2\left(\frac{\gamma}{(1-\gamma)^4}\right)=0 \tag{13b}$$

Eliminating HV^2 in Equations (12) and (13), the nonlinear equation of motion about the critical tilting angle for the two cases is:

$$\gamma_{cr}^{\ 3}-3\gamma_{cr}(1-\gamma_{cr})^2\left(\frac{\gamma_{cr}}{1-\gamma_{cr}}+\ln(1-\gamma_{cr})\right)=0 \tag{14a}$$

$$\gamma_{cr}^{\ 3}-\frac{3}{4}\gamma_{cr}(1-\gamma_{cr})^4\left\{\left[\frac{\gamma_{cr}}{1-\gamma_{cr}}+\ln(1-\gamma_{cr})\right]-\left[\frac{-\gamma_{cr}}{1+\gamma_{cr}}+\ln(1+\gamma_{cr})\right]\right\}=0 \tag{14b}$$

Substituting γ_{cr} into Equations (12a) and (12b), the value of critical voltage for single and double electrode actuation can be rewritten respectively as:

$$V_{cr}=\left\{\frac{\gamma_{cr}^{\ 3}}{H\left(\frac{\gamma_{cr}}{1-\gamma_{cr}}+\ln(1-\gamma_{cr})\right)}\right\}^{1/2} \tag{15a}$$

$$V_{cr}=\left\{\frac{\gamma_{cr}^{\ 3}}{H\left[\left[\frac{\gamma_{cr}}{1-\gamma_{cr}}+\ln(1-\gamma_{cr})\right]-\left[\frac{-\gamma_{cr}}{1+\gamma_{cr}}+\ln(1+\gamma_{cr})\right]\right]}\right\}^{1/2} \tag{15b}$$

3. 2. Dynamic Stability Applying harmonic (ac) voltage can affect the stability conditions of the double electrode actuation. In order to investigate the stability of the system governed by Equation (10) and extract the transition curves, $\delta=\delta(\varepsilon)$,the perturbation method based on strained parameters is employed [27]. To this end, equation parameters γ and δ are expanded uniformly in powers of ε:

$$\gamma(\tau;\epsilon)=\gamma_0(\tau)+\epsilon\gamma_1(\tau)+\epsilon^2\gamma_2(\tau)+O(\epsilon^3)$$
$$\delta=n^2+\epsilon\delta_1+\epsilon^2\delta_2+O(\epsilon^3) \tag{16}$$

Upon substituting Equation (16) into Equation (10) and equating the coefficients of like powers of ϵ, following set of equations are obtained:

$$\ddot{\gamma}_0(\tau)+n^2\gamma_0(\tau)=0 \tag{17}$$

$$\ddot{\gamma}_1(\tau)+n^2\gamma_1(\tau)=-\delta_1\gamma_0(\tau)-2\cos(2\tau)\gamma_0(\tau) \tag{18}$$

$$\ddot{\gamma}_2(\tau)+n^2\gamma_2(\tau)=-\delta_1\gamma_1(\tau)-\delta_2\gamma_0(\tau)-2\cos(2\tau)\gamma_1(\tau) \tag{19}$$

$$\ddot{\gamma}_3(\tau)+n^2\gamma_3(\tau)=-\delta_1\gamma_2(\tau)-\delta_2\gamma_1(\tau)-\delta_3\gamma_0(\tau)-2\cos(2\tau)\gamma_2(\tau) \tag{20}$$

Note that in the absence of time-dependent components (ε=0), positive sign of δ corresponds to a stable position of the system, and vice versa. On the other hand, when there is a small time varying component, the system loses to have periodic solution when n is an integer. Therefore, to evaluate the relation between δ and ε (or to draw transition curves), n is assumed as an integer (n=0, 1, 2 …) in the power expansion Equation (16) and the general solution of Equation (17) is as:

$$\gamma_0(\tau) = a\cos(n\tau) + b\sin(n\tau) \tag{21}$$

which yields the bounded solution ($\gamma_0=a$) for (n=0). Substituting this into Equations (18) through (20), while eliminating secular terms following results are obtained:

$$\delta_1 = 0 \ , \ \gamma_1 = \left(\frac{1}{2}\right)a\cos(2\tau)$$
$$\delta_2 = -\frac{1}{2}(a \neq 0, \ for \ nontrivial \ solution), \ \gamma_2 = \left(\frac{1}{32}\right)a\cos(4\tau) \tag{22}$$

Thus, the (δ- ε) relation for ($n=0$) up to the second order reads as:

$$\delta = -\left(\frac{1}{2}\right)\epsilon^2 \tag{21}$$

Transition curve given by Equation (23) and starting from $\delta=0$ specifies the periodic solutions and separates the stable and unstable regions. The same procedure is followed to obtain transition curves for n=1, 2, 3… [27].

4. NUMERICAL RESULTS AND DISCUSSIONS

Simulation results are presented in two separate subsections, where the micro-mirror is excited with some levels of (dc) voltages and superimposing an (ac) component on it. The values of the parameters of the micro-mirror used in the simulations are taken from [22] and listed in Table 1.

TABLE 1. Data used in the simulations

Item	Parameter	Value
Material properties (Silicon)	Shear modulus G (GPa)	66
	Young's modulus, E (GPa)	170.28
	Density, ρ (Kg/m^3)	2,330
Micro-mirror	Width, $2a$ (μm)	100
	Length, L (μm)	100
Torsional micro-beam	Length, l (μm)	65
	Width, w (μm)	2
	Thickness, t (μm)	1.5
Electrode	Width, a (μm)	100
	Gap, D (μm)	2.75

4. 1. Steady Voltage Excitation Fixed points of the micro-mirror in cases of single and double side electrode actuation are depicted in Figure 4. In the double electrode type, for low applied voltages three equilibrium points exist only one of which is stable. For sufficiently high voltages, beyond the Pitchfork bifurcation point, the pull-in phenomena takes place and system possesses only one unstable equilibrium point. In the case of single actuating electrode, there are two equilibrium points one of them is stable and the other unstable for applied voltages lower than the pull-in value. As the applied voltage reaches pull-in value, saddle node bifurcation occurs and the equilibrium points vanish.

In order to gain a better insight of the stability, dynamic response of the system is evaluated for different initial conditions and different applied voltages (Figures 5 and 6). For double electrode actuating, in the absence of bias voltage ($V=0$ *volt*), there exists only one stable center at $\gamma=0$ (Figure 5a). As the system is excited by a step-input voltage, two other unstable equilibrium points (unstable saddle nodes) emerge.

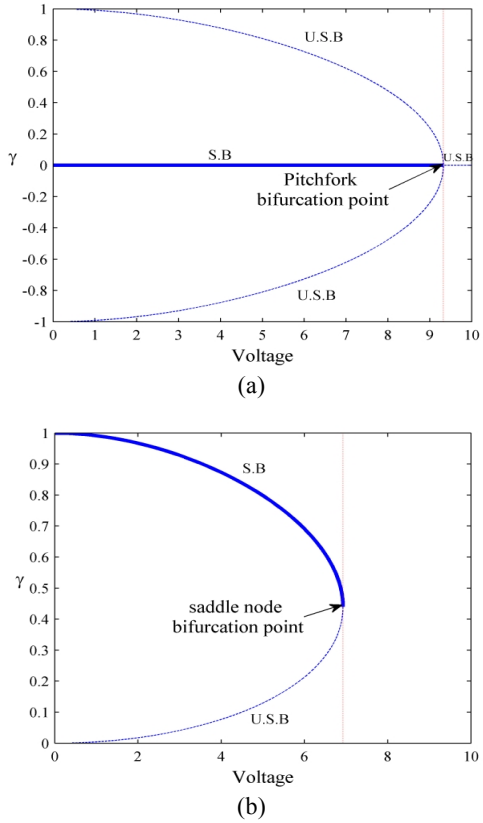

Figure 4. Dimensionless tilting angle of micro-mirror versus applied (dc) voltage, (USB: unstable branch, SB: Stable branch), a) Double electrode actuation. b) Single electrode actuation.

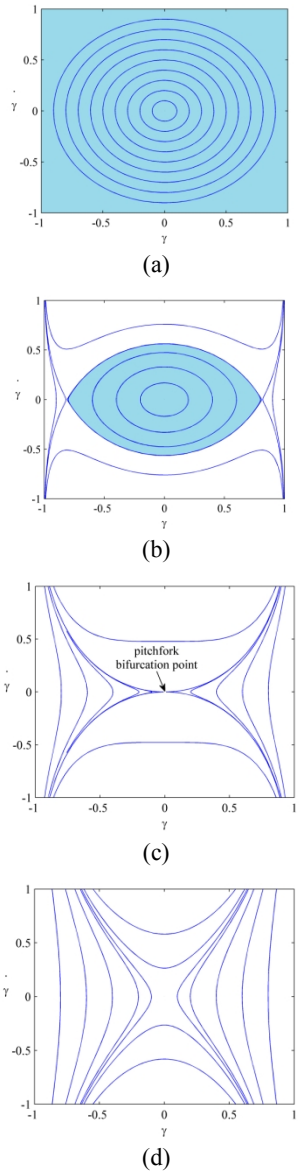

Figure 5. Phase portraits of the double electrode micro-mirror with different initial conditions; (a)V=0 volt, (b) V=5 volt, (c) V_{sp}=9.325 volt, and (d) V=15volt.

Figure 5b shows the basin of attraction of stable center bounded by a homoclinic orbit and basins of repulsion of unstable saddle nodes. As shown in Figure 4a, when the applied voltage approaches a critical value, the stable (S. B) and unstable branches (U. S. B) of the fixed points approach and meet at the pitchfork bifurcation point. The voltage corresponding to this point is known as the static pull-in voltage (V_{sp}) in the MEMS literature. However as the applied voltage increases beyond the pull-in value the basin of attraction of stable attractor is eliminated and the micro-mirror will be unstable for any set of initial conditions (Figures 5c, d).

When the micro-mirror is subjected to single electrode actuation a qualitative changes in the behavior is take placed. In low ranges of applied voltage, the system behavior includes a stable center and an unstable saddle node (Figure 6b). For voltages higher than the pull-in value (which is lower than the pull-in value of double electrode case), the saddle node bifurcation occurs and the attractions no longer exist' Figure 6c and Figure 6d.

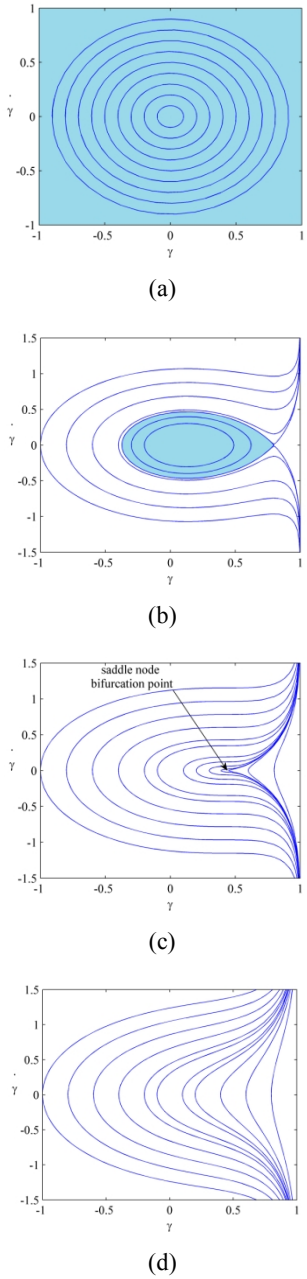

Figure 6. Phase portraits of the single electrode micro-mirror with different initial conditions; (a)V=0 volt, (b) V=5 volt, (c) V_{sp}=6.95 volt, and (d) V=10volt.

4. 2. Parametric Excitations When a harmonic (*ac*) component is superimposed on the applied (*dc*) voltage and symmetrical double electrode actuation is utilized, (Figure 1c), the applied (*dc*) and (*ac*) voltages appear implicitly in the relations containing conventional parameters δ and ε (Equation (9)). The periodic solutions of the Mathieu type Equation (10) is studied in the space δ and ε, and the transition curves are drawn using the perturbation method. Moreover, using δ-ε relations obtained analytically for the transition curves, the stable and unstable regions in the δ-ε plane are illustrated Figure 7. It was proved that along these transition curves there exists at least one normal solution, which is periodic with the period of either 2π or 4π depending on the case. In order to investigate the stability of the specified regions, numerical simulations have been carried out for four specific points located in stable region (*B* and *D*) and unstable region (*A* and *C*). Figure 8 illustrates phase portrait corresponding to point *A* located in the unstable region, where the solution is unbounded. Referring to Equations (9), it can be concluded that this point corresponds to the physical parameters $V_{dc} = 9.1349\, volt, V_{ac} = 0.3806\, volt,\ \Omega = 0.4$

Numerical simulation associated to point *B* in the δ-ε plane is shown in Figure 9. Point *B* is located in the stable region which is substantiated by bounded oscillatory solution. It is noteworthy that an important feature of the proposed parametric analysis is to show the possibility of stabilizing a statically unstable system, where the imposed bias voltage is beyond the pull-in value, by imposing an appropriate alternating voltage. To this end, stability of points C and D is investigated. Figure 10 illustrate phase portrait corresponding to point *C* located in the unstable region, where the solution is unbounded. However, Figure 11 shows that in spite of imposing high (higher than the static pull-in voltage) value as step (*dc*) voltage the system could be stable by superimposing an (*ac*) component. In other words, when the applied (*dc*) voltage is greater than the pull-in value, the system can be stabilized by adding an (*ac*) component with an appropriate amplitude and frequency.

In order to shed light on the effects of the superimposed harmonic voltage, the numerical results related to point *D* is shown again in Figure 12, where sudden removal of the (*ac*) voltage renders the system unstable.

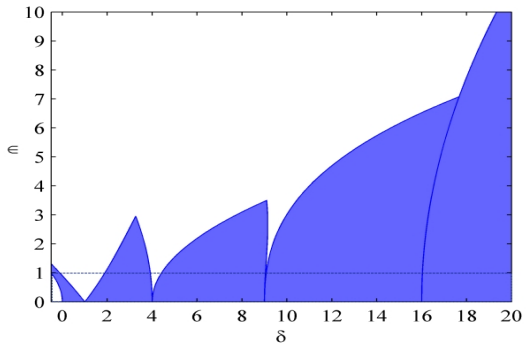

(a)

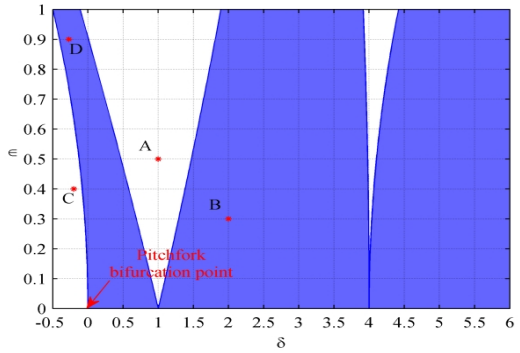

(b)

Figure 7. Stable (shaded) and unstable regions in the parametric plane: (a) $-0.5 < \delta < 20, 0 < \varepsilon < 10$, and (b) $-0.5 < \delta < 6,\ 0 < \varepsilon < 1$

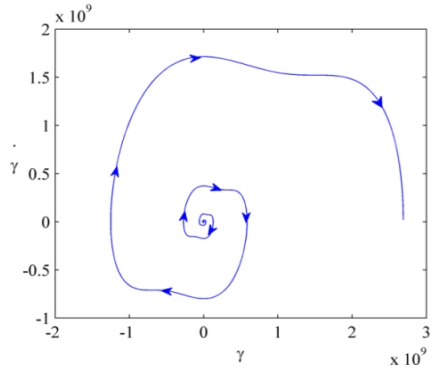

Figure 8. Phase plane associated to point $A(\delta = 1, \epsilon = 0.5)$ equivalent to $(V_{dc} = 9.1349\, volt,\ V_{ac} = 0.3806\, volt,\ \Omega = 0.4)$

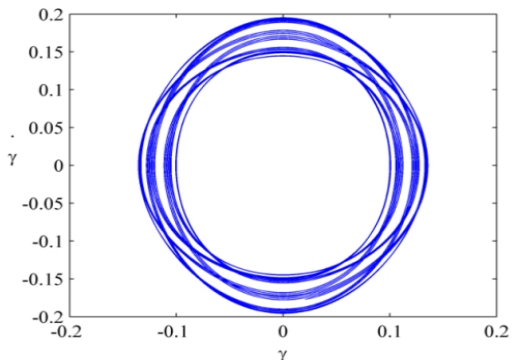

Figure 9. Phase plane associated to point $B(\delta = 2, \epsilon = 0.3)$ equivalent to $(V_{dc} = 8.9425\, volt,\ V_{ac} = 0.2333\, volt,\ \Omega = 0.4)$

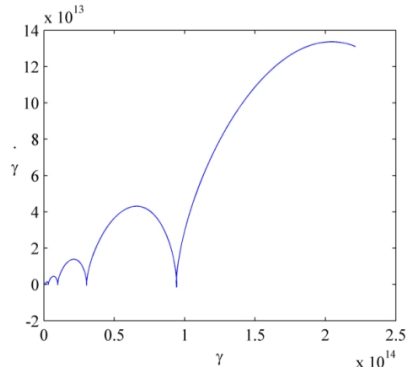

Figure 10. Phase plane associated to point $C\ (\delta = -0.2, \epsilon = 0.4)$ equivalent to $(V_{dc} = 9.3604\ volt,\ V_{ac} = 0.2972\ volt,\ \Omega = 0.4\ )$

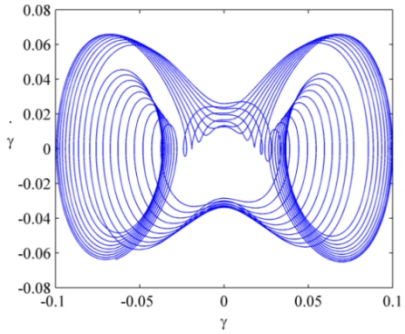

Figure 11. Phase plane associated to point $D(\delta = -0.27, \epsilon = 0.90)$ equivalent to $(V_{dc} = 9.3734\ volt,\ V_{ac} = 0.6677\ volt,\ \Omega = 0.4)$

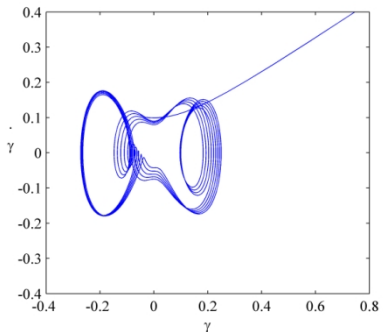

Figure 12. Pull-in instability associated to the point $D(\delta = -0.27, \epsilon = 0.90)$ when the (*ac*) voltage is suddenly removed at *t*=75

It should be noted that the two classical parameters δ and ϵ defining the stability margins or transition curves of the Mathieu type equation depend on the three parameters of the physical problem, V_{dc}, V_{ac} and the dimensionless forcing frequency Ω. In order to estimate the boundaries of the stable regions in terms of explicit excitation characteristics, a nonlinear mapping is carried out from (δ- ε) plane to the (V_{dc}- V_{ac}) plane for given Ω. Figure 13 illustrates the stability regions in (V_{dc}- V_{ac}) plane for different values of dimensionless forcing frequency. The figure gives descriptive results of stability conditions in terms of input voltages. The results show that imposing the (*ac*) component to an unstable system $(V_{dc} > V_{sp} = 9.325)$ can stabilize it, where the (*ac*) amplitude may have a relatively significant value. On the other hand, stabilization of the system at higher (dc) voltages requires higher (*ac*) amplitudes. Furthermore, amplitudes of the (*ac*) voltages increase with increasing the forcing frequency Ω. However, as shown by numerical simulations, despite employing the (*ac*) amplitudes which is not necessarily small, the amplitude of vibrations around the equilibrium position is significantly smaller with respect the distance between the mirror plate and the electrodes.

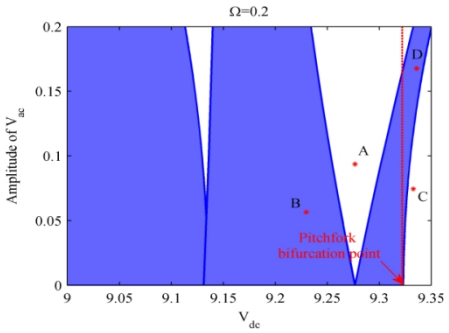

(a)

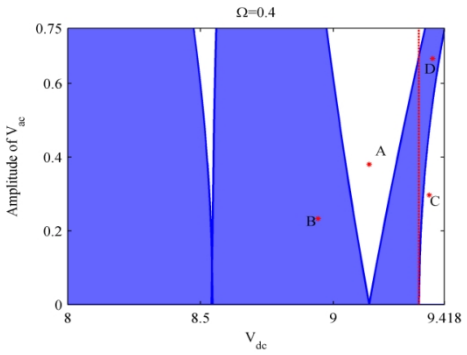

(b)

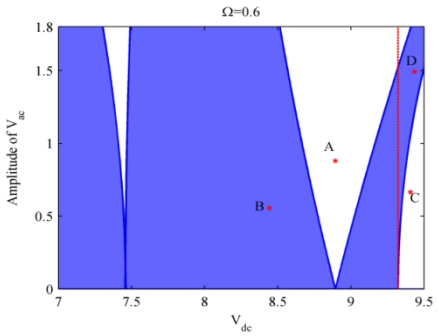

(c)

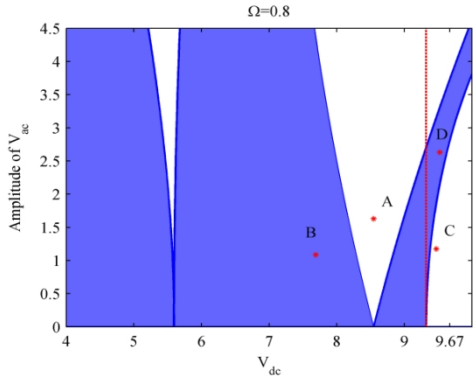

(d)

Figure 13. Stable (shaded) and unstable regions of the system in the plane of forcing parameters (V_{dc}- V_{ac}), (a) Ω=0.2 (b) Ω =0.4 (c) Ω=0.6 6 (d) Ω=0.8

5. CONCLUSION

Electrostatic torsional micro actuators may be excited by a steady (*dc*) or harmonic (*ac*) voltage superimposed on the (*dc*) one or by an electrode or symmetrically double electrodes as well. In this paper, the pull-in conditions of a micro-mirror due to an applied steady (*dc*) voltage were investigated in both types of actuations. When the steady voltage is imposed suddenly, the basins of attractions associated with stable centers are observed. The results show that the system response varied qualitatively in single and double electrode actuations. Assuming double electrode actuation and simultaneously step-input (*dc*) and harmonic (*ac*) voltages, the Mathieu type parametric equation was extracted. The transition curves are plotted in the classical (δ- ε) plane and in the physical problem parameters (V_{ac}- V_{dc}) plane for different forcing frequencies. The correctness of the stable and unstable regions was checked by numerical simulations. The results showed that imposing (*ac*) component on an unstable system (V_{dc}> V_{sp}) can stabilize it. On the other hand, stabilization of the system at higher (*dc*) voltages requires higher (*ac*) amplitudes. Furthermore, it was shown that the amplitude of the (*ac*) voltage increases with increasing the forcing frequency Ω.

6. REFERENCES

1. Hornbeck, L. J., "128× 128 deformable mirror device", ***Electron Devices, IEEE Transactions on***, Vol. 30, No. 5, (1983), 539-545.
2. Muller, R. S. and Lau, K. Y., "Surface-micromachined microoptical elements and systems", ***Proceedings of the IEEE***, Vol. 86, No. 8, (1998), 1705-1720.
3. Lin, T.-H., "Implementation and characterization of a flexure-beam micromechanical spatial light modulator", ***Optical Engineering***, Vol. 33, No. 11, (1994), 3643-3648.
4. Toshiyoshi, H. and Fujita, H., "Electrostatic micro torsion mirrors for an optical switch matrix", ***Journal of Microelectromechanical Systems,*** Vol. 5, No. 4, (1996), 231-237.
5. Dudley, D., Duncan, W. M. and Slaughter, J., "Emerging digital micromirror device (dmd) applications", in Micromachining and Microfabrication, International Society for Optics and Photonics. (2003), 14-25.
6. Toshiyoshi, H., Piyawattanametha, W., Chan, C.-T. and Wu, M. C., "Linearization of electrostatically actuated surface micromachined 2-d optical scanner", ***Journal of Microelectromechanical Systems,*** Vol. 10, No. 2, (2001), 205-214.
7. Dickensheets, D. L. and Kino, G. S., "Silicon-micromachined scanning confocal optical microscope", ***Journal of Microelectromechanical Systems,*** , Vol. 7, No. 1, (1998), 38-47.
8. Wu, W., Li, D., Sun, W., Hao, Y., Yan, G., and Jin, S., "Fabrication and characterization of torsion-mirror actuators for optical networking applications", ***Sensors and Actuators A: Physical***, Vol. 108, No. 1, (2003), 175-181.
9. Lee, K.-N., Shin, D.-S., Lee, Y.-S. and Kim, Y.-K., "Micromirror array for protein micro array fabrication", ***Journal of Micromechanics and Microengineering***, Vol. 13, No. 3, (2003), 474.
10. Syms, R. R., "Surface tension powered self-assembly of 3-d micro-optomechanical structures", ***Journal of Microelectromechanical Systems,*** Vol. 8, No. 4, (1999), 448-455.
11. Fischer, M., Giousouf, M., Schaepperle, J., Eichner, D., Weinmann, M., von Munch, W., and Assmus, F., "Electrostatically deflectable polysilicon micro-mirrors dynamic behavior and comparison with the results from fem modeling with ansys", ***Sens. Actuators A***, Vol. 67, No. 1-3, (1998), 89-95.
12. Bao, M., Sun, Y., Zhou, J. and Huang, Y., "Squeeze-film air damping of a torsion mirror at a finite tilting angle", ***Journal of Micromechanics and Microengineering***, Vol. 16, No. 11, (2006), 2330.
13. Lin, W.-H. and Zhao, Y.-P., "Influence of damping on the dynamical behavior of the electrostatic parallel-plate and torsional actuators with intermolecular forces", ***Sensors***, Vol. 7, No. 12, (2007), 3012-3026.
14. Gusso, A. and Delben, G., "Influence of the casimir force on the pull-in parameters of silicon based electrostatic torsional actuators", ***Sensors and Actuators A: Physical***, Vol. 135, No. 2, (2007), 792-800.
15. Guo, J.-G. and Zhao, Y.-P., "Influence of van der waals and casimir forces on electrostatic torsional actuators", ***Journal of Microelectromechanical Systems,*** Vol. 13, No. 6, (2004), 1027-1035.
16. Guo, J.-G. and Zhao, Y.-P., "Dynamic stability of electrostatic torsional actuators with van der waals effect", ***International Journal of Solids and Structures***, Vol. 43, No. 3, (2006), 675-685.
17. Guo, J.-G., Zhou, L.-J. and Zhao, Y.-P., "Instability analysis of torsional mems/nems actuators under capillary force", ***Journal of Colloid and Interface Science***, Vol. 331, No. 2, (2009), 458-462.
18. Lin, W.-H. and Zhao, Y.-P., "Stability and bifurcation behaviour of electrostatic torsional nems varactor influenced by dispersion

forces", ***Journal of Physics D: Applied Physics***, Vol. 40, No. 6, (2007), 1649.

19. Schenk, H., Dürr, P., Kunze, D., Lakner, H. and Kück, H., "A resonantly excited 2d-micro-scanning-mirror with large deflection", ***Sensors and Actuators A: Physical***, Vol. 89, No. 1, (2001), 104-111.
20. Ping Zhao, J., Ling Chen, H., Ming Huang, J. and Qun Liu, A., "A study of dynamic characteristics and simulation of mems torsional micromirrors", ***Sensors and Actuators A: Physical***, Vol. 120, No. 1, (2005), 199-210.
21. Pandey, A. K. and Pratap, R., "A semi-analytical model for squeeze-film damping including rarefaction in a mems torsion mirror with complex geometry", ***Journal of Micromechanics and Microengineering***, Vol. 18, No. 10, (2008), 105003.
22. Shabani, R., Tariverdilo, S., Rezazadeh, G. and Agdam, A., "Nonlinear vibrations and chaos in electrostatic torsional actuators", ***Nonlinear Analysis: Real World Applications***, Vol. 12, No. 6, (2011), 3572-3584.
23. Azizi, S., Rezazadeh, G., Ghazavi, M.-R. and Khadem, S. E., "Stabilizing the pull-in instability of an electro-statically actuated micro-beam using piezoelectric actuation", ***Applied Mathematical Modelling***, Vol. 35, No. 10, (2011), 4796-4815.
24. Krylov, S., Harari, I. and Cohen, Y., "Stabilization of electrostatically actuated microstructures using parametric excitation", ***Journal of Micromechanics and Microengineering***, Vol. 15, No. 6, (2005), 1188.
25. Rezazadeh, G., Madinei, H. and Shabani, R., "Study of parametric oscillation of an electrostatically actuated microbeam using variational iteration method", ***Applied Mathematical Modelling***, Vol. 36, No. 1, (2012), 430-443.
26. Rhoads, J. F., Shaw, S. W. and Turner, K. L., "The nonlinear response of resonant microbeam systems with purely-parametric electrostatic actuation", ***Journal of Micromechanics and Microengineering***, Vol. 16, No. 5, (2006), 890.
27. Nayfeh, A. and Mook, D., "Nonlinear oscillations. 1979", ***John Willey and Sons, New York***, Vol., No.
28. Şimşek, M., "Fundamental frequency analysis of functionally graded beams by using different higher-order beam theories", ***Nuclear Engineering and Design***, Vol. 240, No. 4, (2010), 697-705.
29. Yang, F., Chong, A., Lam, D. and Tong, P., "Couple stress based strain gradient theory for elasticity", ***International Journal of Solids and Structures***, Vol. 39, No. 10, (2002), 2731-2743.
30. Sadeghian, H., Goosen, H., Bossche, A., Thijsse, B. and van Keulen, F., "On the size-dependent elasticity of silicon nanocantilevers: Impact of defects", ***Journal of Physics D: Applied Physics***, Vol. 44, No. 7, (2011), 072001.
31. Sadeghian, H., Yang, C., Goosen, J., Van Der Drift, E., Bossche, A., French, P., and Van Keulen, F., "Characterizing size-dependent effective elastic modulus of silicon nanocantilevers using electrostatic pull-in instability", ***Applied Physics Letters***, Vol. 94, No. 22, (2009), 221903-221903-3.
32. Li, X., Ono, T., Wang, Y. and Esashi, M., "Ultrathin single-crystalline-silicon cantilever resonators: Fabrication technology and significant specimen size effect on young's modulus", ***Applied Physics Letters***, Vol. 83, No. 15, (2003), 3081-3083.
33. Namazu, T., Isono, Y. and Tanaka, T., "Evaluation of size effect on mechanical properties of single crystal silicon by nanoscale bending test using afm", ***Microelectromechanical Systems, Journal of***, Vol. 9, No. 4, (2000), 450-459.
34. Gordon, M. J., Baron, T., Dhalluin, F., Gentile, P. and Ferret, P., "Size effects in mechanical deformation and fracture of cantilevered silicon nanowires", ***Nano Letters***, Vol. 9, No. 2, (2009), 525-529.
35. Sadeghian, H., Yang, C.-K., Goosen, J. F., Bossche, A., Staufer, U., French, P. J., and van Keulen, F., "Effects of size and defects on the elasticity of silicon nanocantilevers", ***Journal of Micromechanics and Microengineering***, Vol. 20, No. 6, (2010), 064012.

Stability Analysis in Parametrically Excited Electrostatic Torsional Micro-actuators

B. Abbasnejad, R. Shabani, G. Rezazadeh

Mechanical Engineering Department, Urmia University, Urmia, Iran

P A P E R I N F O

Paper history:
Received 06 June 2013
Received in revised form 13 August 2013
Accepted 22 August 2013

Keywords:
MEMS
Micro-mirror
Electrostatic Actuation
Parametric Oscillation
Perturbation Method

چکیده

در این مقاله پایداری استاتیکی و دینامیکی یک میکروآینه در شرایط تحریک پارامتریک مورد بررسی قرار گرفته است. سیستم مورد نظر شامل یک میکروآینه است که به صورت متقارن در بین دو الکترود از نوع تحریک الکترواستاتیک قرار گرفته و به صورت هم‌زمان توسط یک ولتاژ ثابت و یک ولتاژ هارمونیک تحریک می‌شود. در ابتدا با اعمال ولتاژ ثابت، پایداری استاتیکی سیستم بررسی، و ولتاژ ناپایداری، نقاط تعادل و نقاط دوشاخگی سیستم استخراج شده‌اند. سپس، با اضافه کردن ولتاژ متناوب به ولتاژ ثابت، معادله حاکم بر سیستم که به فرم معادله ماتیو می‌باشد استخراج و پایداری سیستم بررسی شده است. در ادامه، با تغییر پارامترهای تحریک سیستم نظیر اندازه ولتاژ ثابت و دامنه ولتاژ تناوبی منحنی‌های گذر و نواحی پایدار میکروآینه مشخص شده‌اند. نتایج به دست آمده از روش اغتشاشات برای نقاط خاص به صورت عددی نیز حل شده و پایداری سیستم به صورت موردی بررسی شده است. نتا یج نشان می‌دهند که با افزودن یک مولفه هارمونیک می‌توان ولتاژ ناپایداری سیستم را افزایش داده و به مقدار بالاتر از ناپایداری استاتیکی نیز رساند. منحنی‌های گذر و نواحی پایدار به دست آمده می‌توانند در طراحی و ساخت میکروآینه‌ها به کار گرفته شوند..

doi: *10.5829/idosi.ije.2014.27.03c.17*